Cell. Mol. Life Sci. 66 (2009) 1729 – 1740
1420-682X/09/101729-12
DOI 10.1007/s00018-009-9145-z

Cellular and Molecular Life Sciences

Research Article

Calmodulin-associated post-translational regulation of rat organic cation transporter 2 in the kidney is gender dependent

S. Wilde[a], E. Schlatter[a], H. Koepsell[b], B. Edemir[a], S. Reuter[a], H. Pavenstädt[a], U. Neugebauer[a], R. Schröter[a], S. Brast[a] and G. Ciarimboli[a,] *

[a] Medizinische Klinik und Poliklinik D, Experimentelle Nephrologie, Universitätsklinikum Münster, Domagkstraße 3a, 48149 Münster (Germany), Fax: +49-251-8356973, e-mail: gciari@uni-muenster.de
[b] Institut für Anatomie und Zellbiologie, Universität Würzburg, Koellikerstrasse 6, 97070 Würzburg (Germany)

Received 26 February 2009; accepted 16 March 2009
Online First 31 March 2009

Abstract. In this work, regulation of organic cation transporter type 2 from rat (rOCT2) stably transfected in HEK293 cells was investigated by microfluorimetry with 4-(4-(dimethylamino)styryl)-N-methylpyridinium as substrate. The transport mediated by rOCT2 was specifically stimulated by PKA, phosphatidylinositol-3-kinase, $p56^{lck}$ tyrosine kinase, mitogen-extracellular-signal-regulated-kinase-1/2, calmodulin (CaM), and CaM-kinase-II. The regulatory pattern of rOCT2 differs markedly quantitatively and qualitatively from that of other OCT isoforms. Only CaM-dependent upregulation is conserved throughout the OCT family. For this reason, CaM regulation of rOCT2 was also investigated in isolated S3-segments (known to express only rOCT2) of male and female rat proximal tubules. Inhibition of CaM by calmidazolium significantly decreased rOCT2 activity ($-49.0 \pm 13.6\,\%$, $n = 4$) in male but not female ($9.0 \pm 13.0\,\%$, $n = 4$) rats. Real-time PCR and Western blot investigations of CaM expression in rat kidneys showed that male animals have significantly higher CaM expression. This is the first study describing post-translational gender-dependent rOCT2 regulation.

Keywords. Organic cation transporter, physiology, regulation, kidney, gender dependence.

Introduction

Organic cation transporters (OCTs) are membrane proteins that have important physiological, pharmacological, and toxicological implications because of their role in the transport of endogenous organic cations, such as the dopaminergic neuromodulators histidyl-proline diketopiperazine and salsolinol [1], histamine [2] and xenobiotica such as metformin [3], platin-derivatives [4–6] and paraquat [7]. The transport mediated by OCTs has been characterized as polyspecific, bidirectional and electrogenic [8]. Three OCT-isoforms (OCT1, OCT2 and OCT3), mainly expressed in epithelia of intestine, liver, brain and kidney in a species- and isoform-specific fashion, have been identified in rat, mouse and man [9]. Common structural properties of OCTs are the presence of 12 putative α-helical transmembrane domains (TMD) with a large hydrophilic extracellular loop between TMD1 and TMD2 and a big intracellular loop between TMD6 and TMD7 containing several potential protein kinase phosphorylation sites [10].

The rat OCT2 (rOCT2, also called solute carrier 22a2) is mainly expressed in the kidney at the basolateral membrane of S2 and S3 segments of the proximal

* Corresponding author.

tubule in the outer stripe of the outer medulla [11, 12]. Rat OCT1 is also highly expressed in the kidney, but it is localized at the basolateral membrane of S1 and S2 segments of superficial and juxtamedullary proximal convoluted tubules [13]. The human kidney expresses mainly the hOCT2 isoform on the basolateral cell membrane of the entire proximal tubule [14].

Compared to female rats, males have a higher expression of rOCT2 both at mRNA and protein levels, which is dependent on testosterone [15, 16]. Androgen response elements (AREs) in the 5′-flanking region of the rOCT2 gene are responsible for stimulation of rOCT2 promoter activity by testosterone [17].

Although regulation of different OCT isoforms has been extensively studied [18–22], there is no information available about regulation of rOCT2. Since the rat is a commonly used animal model for physiological, pharmacological and toxicological studies, in this work the properties of rOCT2 expressed in HEK-293 cells, with special emphasis on its regulation by different intracellular pathways, were investigated. Furthermore, the gender-dependency of regulation was also examined in freshly isolated rat proximal tubular S3 segments from male and female rats.

Materials and methods

HEK293 Cell culture. Experiments were performed with human embryonic kidney (HEK)-293 cells (CRL-1573; American Type Culture Collection, Rockville, MD), which stably express rOCT2 or rOCT1. rOCT2 or rOCT1 was cloned and stable transfection was performed as described earlier [23, 24]. Cells were grown at 37 °C in 50 ml cell culture flasks (Greiner, Frickenhausen, Germany) in DMEM (Biochrom, Berlin, Germany) containing 3.7 g/l $NaHCO_3$, 1.0 g/l D-glucose, and 2.0 mM L-glutamine (Biochrom), and gassed with 8% CO_2. Penicillin (100 U/ml), 100 mg/l streptomycin (Biochrom), 10% fetal calf serum, and, only for OCT-transfected cells, 0.8 mg/ml geneticin (PAA Laboratories, Coelbe, Germany) were added to the medium. Experiments were performed with confluent cells grown on glass coverslips for 5–8 days or in 96-well-microplates for 2–3 days from passages 12–90. No difference in the time at which confluency was reached was noted over this broad range of passages. Moreover, to check for reproducibility of the experiments with cells of different passages, the effects of substances such as forskolin, 8-Br-cGMP, and aminogenistein were periodically tested. Each set of experiments was performed on the same day with cells of the same age and passage. Culture and functional analyses of these cells were approved by the state government Landesumweltamt Nordrhein-Westfalen, Essen, Germany (no. 521.–M-1.14/00).

Isolation of tubular segments for microfluorimetry. Lewis–Brown–Norway (LBN) rats (240–290 g, Charles River, Sulzfeld, Germany) with free access to standard rat chow (Ssniff, Soest, Germany) and tap water were used. Experiments were approved by a governmental committee on animal welfare and were performed in accordance with national animal protection guidelines. Proximal tubules (S3 segments) were mechanically isolated in MEM-EARLE medium (Biochrom), transferred to a perfusion chamber, and fixed by two holding pipettes closing the lumina at the ends of the tubule segment for microfluorimetric measurements. In this way, only the basolateral side of the tubules, where rOCT2 is located [12], could be reached by the experimental solutions.

Fluorescence measurements. As substrate for OCTs, the fluorescent organic cation 4-(4-(dimethylamino)styryl)-N-methylpyridinium (ASP^+) at a concentration of 1 μM was used. The ASP^+-uptake by rOCT2 expressing cells was measured by two methods:

Method 1. The fluorescence measurement device and experimental procedures used in this method were already described in detail [18, 20, 25]. Measurements were performed in the dark with an inverted microscope (Axiovert 135; Zeiss, Oberkochen, Germany) equipped with a 100x oil immersion objective. Excitation light (450 to 490 nm) was reflected by a dichroic mirror (560 nm) to a perfusion chamber. Cell monolayers on cover slips formed the bottom of the chamber. The preparations were superfused at a rate of 10 ml/min with a HCO_3^- free Ringer-like solution containing (in mmol): NaCl 145, K_2HPO_4 1.6, KH_2PO_4 0.4, D-glucose 5, $MgCl_2$ 1, calcium gluconate 1.3, and pH adjusted to 7.4 at 37 °C. Fluorescence emission (575 to 640 nm) was measured by a photon counting tube (Hamamatsu H 3460–04; Herrsching, Germany). To directly determine the affinity of rOCT2 for ASP^+, saturation experiments at 37 °C and 8 °C were performed as already described [26]. This approach was also used to determine K_m and V_{max} under the regulatory influence of calmodulin inhibition. To study regulation of rOCT2, ASP^+-uptake was evaluated after incubation with the respective agonists or inhibitors in the continued presence of these substances and compared to that observed in control experiments performed under the same conditions without agonists or inhibitors. Results are expressed as changes of ASP^+-uptake in percentage of control experiments.

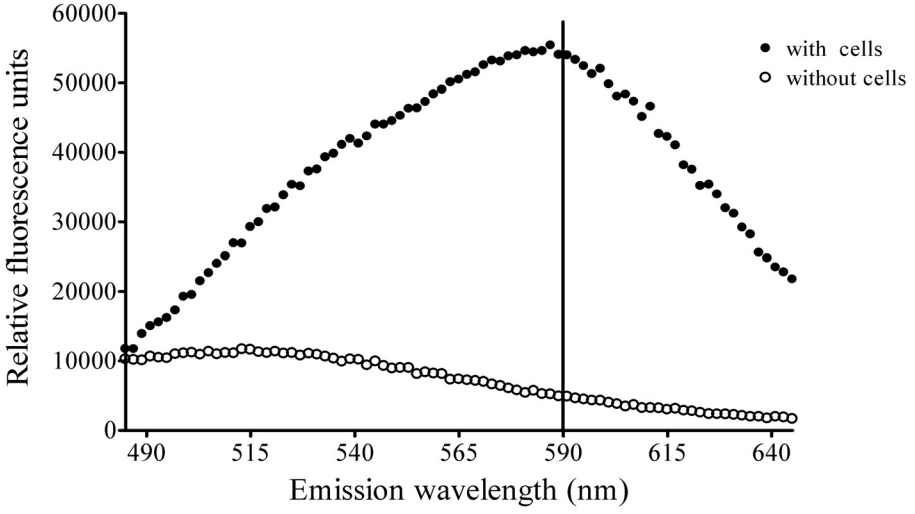

Figure 1. Emission spectrum of ASP^+ (1 μM) at an excitation wavelength of 450 nm in wells with (closed circles) or without (open circles) rOCT2-expressing HEK-293 cells. The vertical line indicates the wavelength chosen for fluorescent emission readings.

Method 2. Taking advantage of the shift in the emission spectrum of ASP^+ when taken up by the cells (Fig. 1), the microfluorimetric detection of ASP^+-uptake has been adapted to obtain a high throughput measurement platform using a fluorescent plate reader (Infinity M200, Tecan, Crailsheim, Germany). Other known fluorescent substrates for OCTs that do not show such an emission spectrum shift, as, e. g. amiloride, are not suitable as substrate in this application (data not shown). Briefly, cells confluently grown on 96-well-microplates (Nunclon 96 Flat bottom, Nunc, Wiesbaden, Germany) were excited with monochromatic light of 450 nm and fluorescence emission, filtered by a second monochromator at 590 nm, was finally measured by a fluorescence detector. Fluorescence was measured in each well before and after ASP^+-injection. The IC_{50} values for inhibition of ASP^+ uptake by other organic cations obtained with this technique were not different from those obtained with method 1 (not shown). When investigating regulation pathways, an incubation step with the respective agonists or inhibitors was added. Also in this case, initial results obtained with method 1 and method 2 were the same (not shown). The regulation effects reported here were determined with method 2. All experiments were performed at 37 °C.

ASP^+-uptake in isolated S3 segments of rat proximal tubules. Experiments with freshly isolated proximal tubules were performed as already described for human tubules [25]. Briefly, dynamic fluorescence microscopy with isolated tubules was performed in the dark at 37 °C with an inverted microscope (Axiovert 135, Zeiss, Oberkochen, Germany) equipped with a 100 x 1.45 oil-immersion objective. Data acquisition and analysis were performed with Metafluor Software (Visitron Systems, Puchheim, Germany). Excitation light (488 nm) from a polychromator system (VisiChrome, Visitron Systems, Puchheim, Germany) was reflected to the tubules by a dichroic mirror (560 nm) and emission was detected after passing an emission filter (575–640 nm) by a Photometrics $CoolSNAP_{EZ}$ digital camera (Roper Scientific, Tuscon, USA). The intensity of signal per region of interest across the basolateral membrane of the tubules was corrected by subtracting the intensity of background signal as determined in a tubule-free region of the same size and area.

In all fluorescent measurements, the initial linear slope of cellular fluorescence increase during the first 10 to 40 s was used as the transport parameter. This initial fluorescence increase directly represents the ASP^+ uptake across plasma membranes via OCTs and is not significantly influenced by transport of ASP^+ out of the cells, intracellular compartmentalization and bleaching of the dye [27]. Since the technical conditions of the experiments vary with time (for example the intensity of the light source decreases with time), it is not possible to compare experiments using absolute values. For this reason, the results are expressed as percentage of control experiments performed on the same day with cells of the same passage and age or in the same tubules.

Real time PCR. Gene expression profiles were analyzed by real time PCR. Total RNA from male and female LBN rat whole kidneys or S3-segments of proximal tubules were isolated using RNeasy-kit (Qiagen, Hilden, Germany). The S3-segments were isolated according to the procedure described by Schafer et al. [28]. For cDNA synthesis, 2 μg total RNA was used with the SuperScript-III First-Strand Synthesis SuperMix (Invitrogen, Carlsbad, CA, USA). Real time PCR was performed using SYBR

Table 1. Sequences of primers used for real time PCR

Gene description and acc. no.	Primer sequences
Rattus norvegicus calmodulin 1 NM_031969.2	Sense-ACCTCGGGGAAAAGCTAACAGATG Antisense-GGTCTTCATTTTGCAGTCATCATC
Rattus norvegicus solute carrier family 22, member 2 (Slc22a2) NM_031584	Sense-GCAAGCAGACCGTCCGCTAAG Antisense-CAGACCGTGCAAGCTACAGCAC
Rattus norvegicus glyceraldehyde-3-phosphate dehydrogenase (Gapdh) NM_017008	Sense- CATCAACGACCCCTTCATT Antisense- ACTCCACGACATACTCAGCAC

Green PCR Master Mix on an ABI PRISM 7700 Sequence Detection System. Specific primer pairs as listed in Table 1 were used. All instruments and reagents were purchased from Applied Biosystems (Darmstadt, Germany). Relative gene expression values were evaluated with the $2^{-\Delta\Delta Ct}$ method using Gapdh as housekeeping gene [29].

Western blot analyses. For Western blot analyses, proteins from whole kidney lysates were separated by SDS-polyacrylamide (4–20 %) electrophoresis and transferred to a PVDF membrane incubated with 3 % gelatine as a blocking agent. After incubation with the primary antibody against calmodulin (rabbit polyclonal calmodulin antibody, Cell Signaling Technology, Danvers, MA, USA), membranes were incubated with a peroxidase-conjugated anti-rabbit secondary antibody and signals visualized by super signal cheminoluminescent detection (Perbio Science, Bonn, Germany). Semi-quantification of specific signals and the internal standard ß-tubulin (Sigma, Taufkirchen, Germany) blotted in parallel was performed using the BioDoc analysis software (Biometra, Göttingen, Germany).

Chemicals. 8-Bromo 3′,5’ -cyclic guanosine monophosphate (8-Br-cGMP), forskolin, quinine hydrochloride, corticosterone, tetraethylammonium (TEA^+), tetrapenthylammonium (TPA^+), cimetidine, rapamycin and N-amidino-3,5-diamino-6-chloropyrazine-carboxamide (amiloride) were obtained from Sigma (Taufkirchen, Germany). Aminogenistein, calmidazolium, sn-1,2-dioctanoyl glycerol (DOG), 1-[N,O-bis-(5-isoquiolinesulfonyl)- N-methyl-L-tyrosyl]-4-phenylpiperazine (KN62), 1,4-diamino-2,3-dicyano-1,4-bis(2-aminophenylthio)-butadiene (UO126), KT5823, KT5720, 1-(5-iodonapthalene-1-sulfonyl) homopiperazine (ML-7), and wortmannin were purchased from Calbiochem (Bad Soden, Germany). ASP^+ was purchased from Molecular Probes (Invitrogen, Karlsruhe, Germany). All other substances and standard chemicals were obtained from Sigma or Merck (Darmstadt, Germany). Compounds were dissolved in HCO_3^- free Ringer like solution and if necessary with ethanol or dimethylsulphoxide (DMSO) as solvent. The final concentration of these solvents did not affect the results of the experiments (data not shown).

Statistical Analyses. Data are presented as mean values ± SEM, with (n) referring to the number of monolayers, wells, or tubules. K_m, V_{max} and IC_{50} values were obtained by sigmoidal concentration-response curve fitting (constant Hill-slope) using GraphPad Prism, Version 4.0 (GraphPad Software, Inc., San Diego, USA). Unpaired two-sided Student’s t-test was used to prove statistical significance of the effects. When indicated, ANOVA with Tukey posthoc test was applied. A P-value < 0.05 was considered statistically significant.

Results

Transport properties of rOCT2 stably expressed in HEK293 cells. As shown in Figure 2, the uptake of ASP^+ in rOCT2 expressing cells increased in a concentration-dependent manner and was temperature-dependent. At a concentration of 1 μM, the ASP^+ uptake at 8 °C was around 10 % of that observed at 37 °C, corresponding to the maximal effect of inhibitors on the uptake of 1 μM ASP^+ (see below and Fig. 3). However, the ASP^+ uptake at 8 °C showed a linear increase with higher ASP^+ concentrations (Fig. 2). As the temperature-dependent uptake of ASP^+ (determined by subtracting ASP^+-uptake measured at 8 °C from that measured at 37 °C) reached saturation (Fig. 2), K_m and V_{max} values could be determined (K_m = 7 μM; V_{max} = 203 photons/s^2). The K_m value is in the same concentration range as that observed for hOCT2 (24 μM) using the same technique [26].

To validate measurements obtained with the high throughput fluorescent plate reader (method 2), in preliminary experiments IC_{50} values for TEA^+, TPA^+, and quinine were obtained in parallel with our previously used fluorescence device (method 1). Results were always identical and therefore only

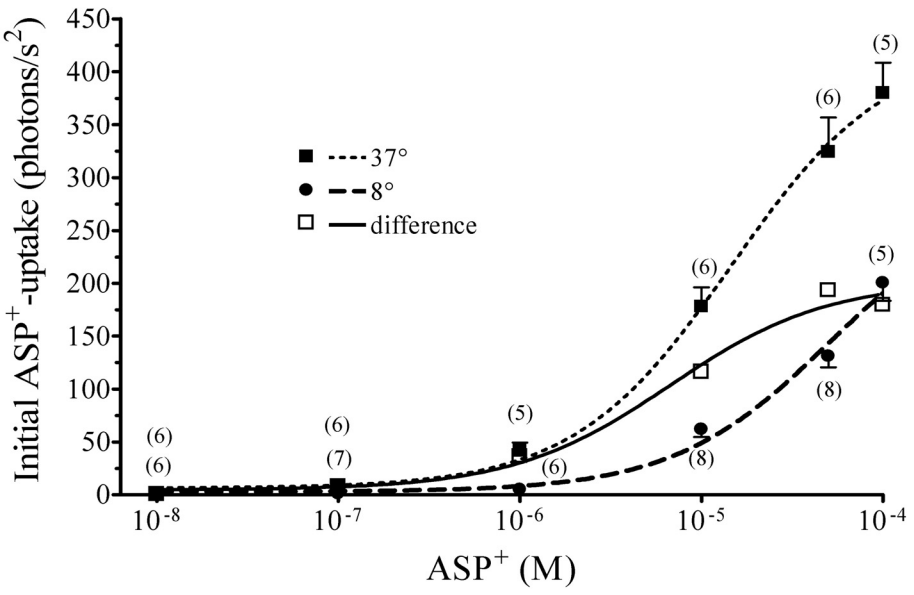

Figure 2. Comparison of ASP^+-uptake in rOCT2 expressing cells at the physiological temperature of 37 °C (small dotted curve) with the uptake at 8 °C (dashed curve). The continuous black curve is the temperature-dependent ASP^+-uptake by rOCT2, calculated as difference between uptake at 37 °C and 8 °C ($K_m = 7$ μM; $V_{max} = 203$ photons/s^2). Values are means ± SEM with number of observation in parentheses.

results obtained with method 2 are presented. When performing a concentration-dependent inhibition curve with these substances, several microtiter plates, where different concentrations of the inhibitor were tested, were used. In order to be able to compare the results from different plates, control measurements were run in every plate, resulting in a high number of control measurements (86, 64, and 64 for TEA^+, TPA^+, and quinine, respectively) and, consequently, in a broad range of experiment numbers. Substrate specificity of rOCT2 was investigated by studying inhibition of ASP^+-uptake by known substrates and inhibitors of organic cation transport, like TPA^+, TEA^+, cimetidine, quinine and corticosterone [30]. TPA^+, TEA^+, cimetidine, quinine and corticosterone inhibited ASP^+-uptake concentration-dependently, with IC_{50} values of 1.3, 176, 23, 24, and 0.8 μM, respectively (Fig. 3). Since corticosterone has been described as a non-transported inhibitor of rOCT2 [31] and as binding rOCT2 with a much higher affinity compared with rOCT1 [24], the effects of corticosterone on rOCT2- and rOCT1-mediated transport were compared. A concentration of 10 μM corticosterone significantly inhibited (-85 ± 2 %, n = 12) the rOCT2-mediated ASP^+-uptake, but had no effect on transport mediated by rOCT1 (not shown). This corticosterone concentration was therefore used to confirm that the ASP^+-uptake observed in experiments with the freshly isolated rat kidney tubules was mediated by rOCT2 (see below).

Regulation of rOCT2. Since the kidney is the target of many hormones that can activate a series of regulation pathways (See [10]), we examined the effects of enzymes physiologically activated by stimulation of G-protein coupled receptors (PKA, PKC, phosphatidylinositol-3-kinase) and ANP-receptors (PKG) on transport mediated by rOCT2. Moreover, we have also investigated the influence of calmodulin and of $p56^{lck}$ tyrosine kinase signaling pathway on rOCT2 activity. These two enzymes have been already shown to regulate other OCT isoforms (See below and [20, 22, 26, 27]).

Activation of the cAMP dependent protein kinase PKA by 10 minute incubation with 1 μM forskolin caused a slight but significant stimulation of ASP^+-uptake (+11.0 ± 3.8 %, n = 83; Fig. 4). Simultaneous incubation with forskolin and the PKA inhibitor KT5720 (1 μM) suppressed this stimulation (+0.8 ± 5.2 %, n = 16), demonstrating the specificity of the effect. KT5720 alone had no significant effect on ASP^+-uptake (-6.2 ± 6.4 %, n = 16; Fig. 4). A similar effect upon PKA-stimulation (approximately 20 % stimulation) had also been observed measuring [^{3}H]TEA^+-uptake in CHO-K1 cells stably transfected with rbOCT2 [21]. A stronger activation of the ASP^+-transport (about 51 %) had been observed in HEK 293 cells expressing the rOCT1 [18], while in HEK 293 cells expressing hOCT2 stimulation of PKA had an inhibitory effect on transporter activity [26]. These results suggest that the PKA-regulation is species-dependent and differs between the OCT isoforms.

To examine whether ASP^+-uptake is influenced by the activity of PKC, cells were incubated for 10 minutes with the PKC activator DOG, which is a membrane-permeable analogue of diacylglycerol. The effect of DOG (1 μM) on ASP^+ transport did not reach significance (change of ASP^+-uptake compared to control: +10.0 ± 4.0 %, n = 40). This DOG concentration has been already shown to exert significant

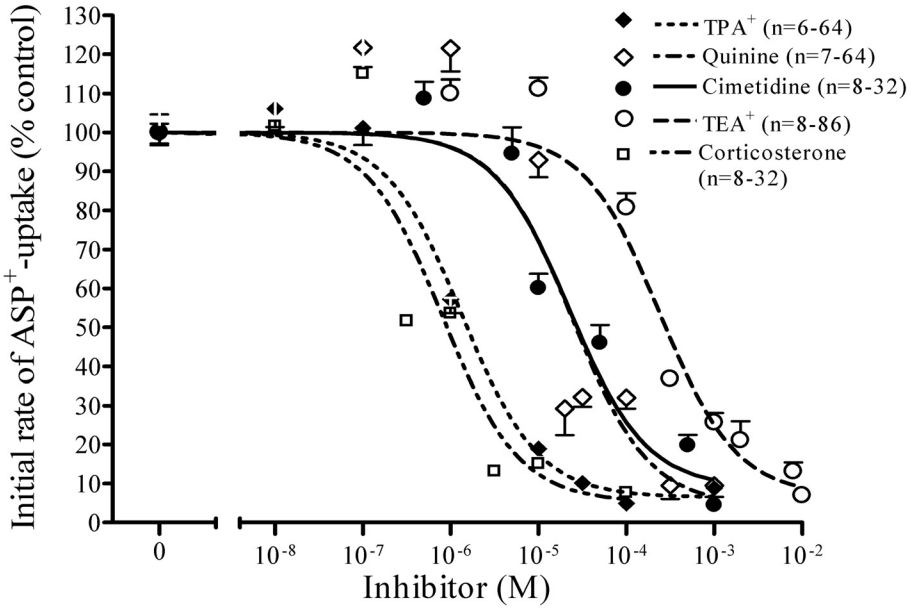

Figure 3. Concentration-response curves for the inhibition of initial ASP^+-uptake by TEA^+, TPA^+, quinine, cimetidine and corticosterone. Values are means ± SEM expressed as % ASP^+-uptake in the absence of the inhibitor with number of observation in parentheses. IC_{50} values determined from these curves were 176 (TEA^+), 1.3 (TPA^+), 24 (quinine), 23 μM (cimetidine), and 0.8 μM (corticosterone).

regulatory effects on the ASP^+-uptake by rOCT1 (around 90% increase [27]), and hOCT2 (around 30% decrease [26]) stably expressed in HEK293 cells. ASP^+-uptake was not significantly influenced by incubating cells with 100 μM 8-Br-cGMP, a membrane-permeable analogue of cGMP which activates PKG (-7.4 ± 1.6%, n = 44), in contrast to that observed in rOCT1 and hOCT2 [32]. Also hOCT1 and hOCT3 were not regulated by this pathway [20, 22]. Since a threonine with characteristics of a potential PKG-phosphorylation site at position 348–351 is present in all these transporters, these results suggest that the effects observed in rOCT1 and hOCT2 are not mediated by a direct interaction of PKG with the transporters [32].

Incubation with the $p56^{lck}$ tyrosine kinase inhibitor aminogenistein (5 μM, 10 min) significantly reduced ASP^+-uptake in rOCT2 cells (-14.7 ± 2.6%, n = 48; Fig. 5). This pathway is also involved in rOCT1 [18] regulation, even though for this isoform effects are much stronger than for rOCT2. Interestingly, inhibition of $p56^{lck}$ tyrosine kinase did not significantly change the hOCT2-mediated ASP^+-transport (Ciarimboli, unpublished results), showing another significantly different regulation between human and rat OCT2.

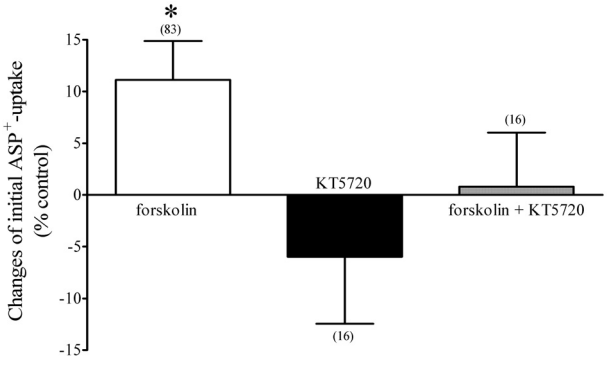

Figure 4. Regulation of rOCT2-mediated ASP^+-transport by PKA-stimulation with forskolin. Cells were incubated at 37 °C for 10 min with forskolin (1 μM) or KT5720 (1 μM) or with a combination of both. Initial uptake rates of ASP^+ after incubation with these different effectors are presented in % uptake of controls. Values are means ± SEM of initial fluorescence increase with number of cell monolayers in parentheses; * indicates statistically significant effects ($P < 0.05$).

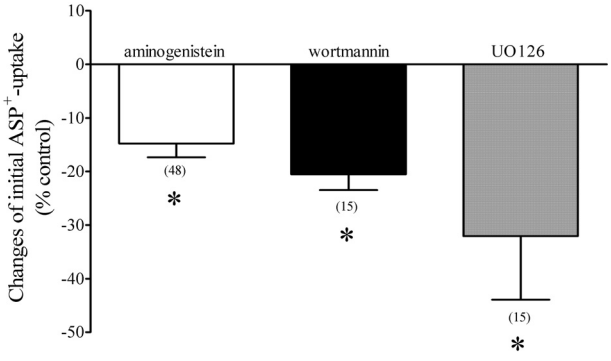

Figure 5. Regulation of rOCT2-mediated ASP^+-transport by inhibition of $p56^{lck}$ tyrosine kinase with aminogenistein (5 μM), of PI3K with wortmannin (0.1 μM), and of MEK1 and MEK2 with UO126 (1 μM). Cells were incubated at 37 °C for 10 min with the respective regulator. Initial uptake rates of ASP^+ after incubation with these different effectors are presented in % uptake of controls. Values are means ± SEM of initial fluorescence increase with number of cell monolayers in parentheses; * indicates statistically significant effects ($P < 0.05$).

Since activation of PI3K is a common pathway of G-protein-coupled receptor and receptor tyrosine kinase activation [33], we tested whether PI3K is involved in the regulation of rOCT2. Ten minute incubation of the cells with wortmannin, a potent inhibitor of PI3K activity, significantly inhibited ASP^+-uptake via rOCT2 (-20.5 ± 3.0 %, n = 15; Fig. 5), showing that this kinase is endogenously active and activates rOCT2. PI3K had also been demonstrated to regulate hOCT2, even though in a different fashion: in this case PI3K inhibition by wortmannin stimulated ASP^+-transport by hOCT2 [19, 26], meaning that this isoform is endogenously inhibited by PI3K. The components of the signaling pathway of G-protein-coupled receptors downstream of PI3K probably are also involved in regulation of rOCT2 activity, because inhibition of the mitogen-activated kinase kinases MEK1 and 2 by 10 min incubation with 1 μM UO126 significantly inhibited ASP^+-transport (-32.1 ± 11.8 %, n = 15; Fig. 5), suggesting that MEK1 and 2 endogenously activate rOCT2, in analogy to what was observed for PI3K. A similar effect had been demonstrated for rbOCT2 [21], while hOCT2 activity was not subject to this regulation [19]. Investigation of rOCT2 regulation by mammalian-target-of-rapamycin (mTOR), a downstream component of the PI3K pathway [34], showed that inhibition of mTOR by 10 min incubation with different rapamycin concentrations (0.1, 1, and 10 μM) had no effect on the rOCT2 activity (not shown).

Inhibition of calmodulin (CaM) by calmidazolium (5 μM, 10 min) significantly reduced ASP^+-transport (-74 ± 2 %, n = 13; Fig. 6a). The regulatory effect of calmodulin seems to be associated rather with a change of K_m (20 vs. 5 μM after 10 min incubation with or without calmidazolium, respectively) rather than with an effect on V_{max} (175 ± 6 vs 190 ± 16 photons/s^2 after 10 min incubation with or without calmidazolium, respectively) (Fig. 6b). To identify possible downstream components of the Ca^{2+}-CaM-mediated regulation of rOCT2, we examined ASP^+-uptake of cells after incubation for 10 minutes with KN-62, an inhibitor of the multifunctional Ca^{2+}-CaM-dependent protein kinase II (CamKII). KN-62 (1 μM) inhibited ASP^+-transport significantly (-35 ± 6 %, n = 12; Fig. 6a). Incubation of rOCT2 cells with KN-62 and calmidazolium simultaneously induced a significant inhibition of ASP^+-uptake (-70 ± 5 %, n = 7), that was not different from that seen using calmidazolium alone (Fig. 6a). Because the Ca^{2+}-CaM complex also activates the myosin light chain kinase (MLCK), the effect of the MLCK inhibitor ML-7 was tested. Ten minutes incubation with ML-7 (3 μM) did not lead to a significant effect on ASP^+-transport (n = 16).

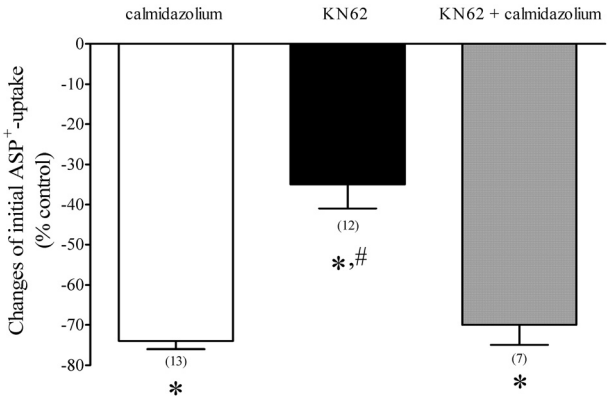

Figure 6a. Regulation of rOCT2-mediated ASP^+-transport by inhibition of CaM with calmidazolium (5 μM), CamKII with KN62 (1 μM) and with a combination of both. Cells were incubated at 37 °C for 10 min with the respective regulator. Initial uptake rates of ASP^+ after incubation with these different effectors are presented in % uptake of controls. Values are means ± SEM of initial fluorescence increase with number of cell monolayers in parentheses; * indicates statistically significant effects from controls (unpaired t-test) and # indicates statistically significant differences from the other groups (ANOVA) ($P < 0.05$).

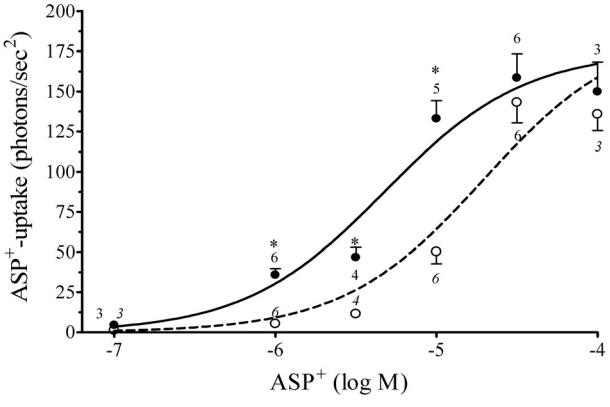

Figure 6b. Effect of inhibition of CaM with calmidazolium (5 μM, 10 min) on K_m and V_{max} of rOCT2. The continuous black curve (closed circles) is the temperature-dependent ASP^+-uptake by rOCT2, calculated as difference between uptake at 37 °C and 8 °C (K_m = 5 μM, 95 % interval of confidence 4 to 6 μM; $V_{max} = 175 \pm 6$ photons/s^2) after 10 min incubation without calmidazolium. The dashed curve (open circles) is the temperature-dependent ASP^+-uptake by rOCT2, calculated as the difference between uptake at 37 °C and 8 °C (K_m = 20 μM, 95 % interval of confidence 12 to 31 μM; V_{max} = 190 ± 16 photons/s^2) after 10 min incubation with calmidazolium. Values are means ± SEM. Number of cell monolayers are indicated in standard and italic types for experiments without and with calmidazolium incubation, respectively; * indicates statistically significant effect differences at single concentrations between the curves with or without calmidazolium incubation (unpaired t-test).

Table 2 summarizes the regulation pathways of rOCT2 identified in this study and compares them with those already described for hOCT2 and rbOCT2 and for the other renal OCT isoform of the rat, rOCT1.

Table 2. Comparison of regulation pathways of rOCT2 as studied in the present work with those of hOCT2 and rbOCT2. The regulation pattern of rOCT1, the other rat renal OCT, is also shown. (↑↑ = strong ≥ 50 %- and ↑ = weak < 50 %-stimulation of the transport activity; ↓ = inhibition of the transport activity; 0 = no effect on the transport activity; n.i. = not investigated; * = Ciarimboli, unpublished results)

	rOCT2	hOCT2	rbOCT2	rOCT1
PKA	↑	↓ [19]	↑ [21]	↑↑ [18]
PKC	0	↓ [19]	n.i.	↑↑ [18]
p56^{lck} tyrosine kinase	↑	0*	n.i.	↑ [18]
cGMP	0	↓ [32]	n.i.	↓ [32]
CaM	↑↑	↑ [19]	n.i.	↑↑*
CamKII	↑	↑ [19]	n.i.	n.i.
MLCK	0	↑ [19]	n.i.	n.i.
PI3K	↑	↓ [19]	n.i.	n.i.
MEK1–2	↑	0 [19]	↑ [21]	n.i.

Regulation of ASP$^+$-uptake by CaM in S3 segments of proximal tubules freshly isolated from rat kidney. The physiological relevance of the most prominent regulation by CaM observed in the expression system has been confirmed by experiments in freshly isolated rat proximal tubules. Addition of corticosterone (10 μM) together with 1 μM ASP$^+$ significantly reduced the ASP$^+$-accumulation in the tubule from male and female animals, confirming the role of rOCT2 in this segment (Fig. 7a and b). In HEK293 cells stably transfected with either rOCT1 or rOCT2, this concentration of corticosterone caused an almost complete inhibition of rOCT2-, while it had no effect on the rOCT1-mediated ASP$^+$-uptake (See above). ASP$^+$-uptake across the basolateral membrane of S3-segments from male and female rat kidney was evaluated before and after incubation with calmidazolium. Figure 7a shows a typical experiment performed with female rat tubules. Incubation with calmidazolium (5 μM) for 10 minutes significantly decreased ASP$^+$-uptake in S3-segments isolated from male but not in those from female rat kidneys (-49.0 ± 13.6 %, n = 4 and +9.0 ± 13.0 %, n = 4, respectively; Fig. 7b).

Calmodulin and rOCT2 expression in male and female kidneys. Calmodulin and OCT2 gene expression in rat kidneys was analyzed by real time PCR using Gapdh expression as internal standard for normalization. Male mRNA expression levels of calmodulin and rOCT2 were set at 100 %. Female expression of calmodulin and rOCT2 was significantly lower compared to male rat kidneys (49 ± 4 %, n = 5, Fig. 8 and 23± 10 %, n = 5 of the expression in males, respectively, not shown). Also in the isolated S3-segments of proximal tubules a lower calmodulin expression in female compared to male rats was observed (50 ± 11 %, n = 3 of the expression in males, Fig. 8). The renal calmodulin expression was also investigated by semi-quantitative Western blot analysis using ß-tubulin as internal standard for quantification (Fig. 9a). Calmodulin protein expression was

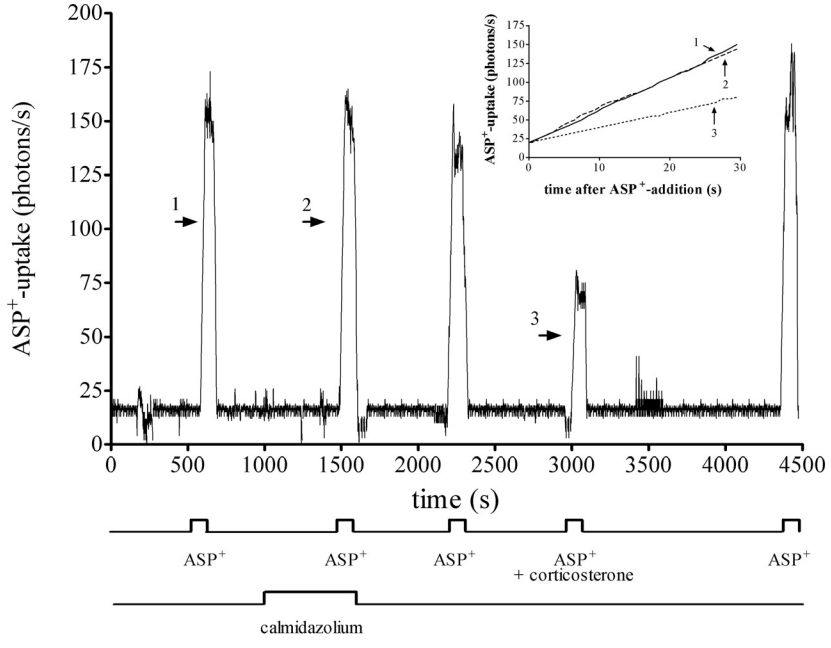

Figure 7a. Example of an experiment where the effect of inhibition of calmodulin by 10 min incubation with calmidazolium (5 μM) in S3-segments of proximal tubules from female rats is tested. The X-axis indicates the time and the Y-axis the fluorescence emission. The first bar below the time axis shows the time of ASP$^+$ pulse addition; the second bar shows incubation with calmidazolium. To clearly illustrate the time course of ASP$^+$-uptake, the insert presents a magnification of the graph representing the fluorescence increase in the first 30 seconds after ASP$^+$-addition. For the sake of clarity, only the curves 1 (control ASP$^+$-uptake), 2 (ASP$^+$-uptake after incubation with calmidazolium), and 3 (ASP$^+$-uptake in the presence of 10 μM corticosterone) are shown.

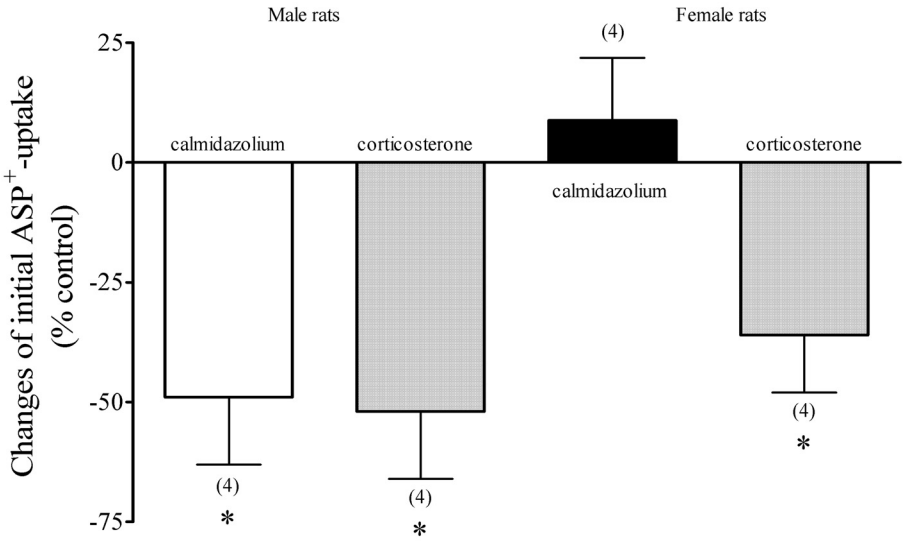

Figure 7b. Effects of inhibition of calmodulin by 10 min incubation with calmidazolium (5 μM) in S3-segments of proximal tubules from male and female rats. Changes of initial uptake rates of ASP^+ are presented in % of control experiments. The effect of 10 μM corticosterone on the ASP^+ uptake is also shown. Values are means ± SEM of initial fluorescence increase with number of tubules in parentheses; * indicates statistically significant effects from controls (paired t-test) ($P < 0.05$).

2.3 times higher in male than in female rat kidneys (Fig. 9b).

Discussion

Since the liver, kidney, and intestine have to deal with rapidly changing amounts of endogenous and exogenous substances as a consequence of variable fluid and food intake as well as metabolic activities, and since in these organs the OCTs are key proteins for the transport of organic cations, an acute regulation of their activity following such various stimuli seems plausible, although the respective coupling mechanism is unknown. The kidney is the target of many hormones that can activate a series of regulation pathways (See [10]).

In this study we demonstrated that rOCT2 is regulated by PKA, PI3K, MEK1 and 2, $p56^{lck}$ tyrosine kinase, CaM and CamKII in corresponding intracellular signalling pathways (Fig. 9) but not by PKG, mTOR, MLCK, and PKC. Compared with rOCT1 [18], the regulation of rOCT2 is qualitatively similar but quantitatively less pronounced. Since rOCT1 is principally localized in S1- and S2- proximal tubules, while rOCT2 is distributed in S2- and S3-segments [12], effects on rOCT1 could represent the bulk of the regulation and those on rOCT2 the fine tuning of transport activity. PKC had been shown to phosphorylate rOCT1 directly, which apparently leads to a conformational change at the substrate binding site [18]. In a previous study it was also demonstrated that all five PKC-phosphorylation sites of rOCT1 are essential for its regulation by PKC [27], suggesting that the special PKC-regulation of rOCT1 is due to its peculiar composition of PKC-phosphorylation sites. Mutations of only one of the five putative PKC-phosphorylation sites of rOCT1 were able to render the transporter insensitive to PKC-regulation [27]. In the rOCT2 only two potential PKC-phosphorylation sites (S286-S553) were identified [10], suggesting that the different effects of PKC-activation on rOCT1 and rOCT2 are indeed linked to the different composition of PKC-phosphorylation sites of the two transporters. Importantly, the rOCT2 regulation also differs from that of hOCT2 [19, 26]: while PKA, PI3K and PKC inhibited the activity of hOCT2, these kinases stimulated (PKA and PI3K) or had no effect (PKC) on rOCT2. MLCK stimulates hOCT2 but is not involved in the rOCT2 regulation. The regulatory effects of a specific regulation pathway in different OCT isoforms

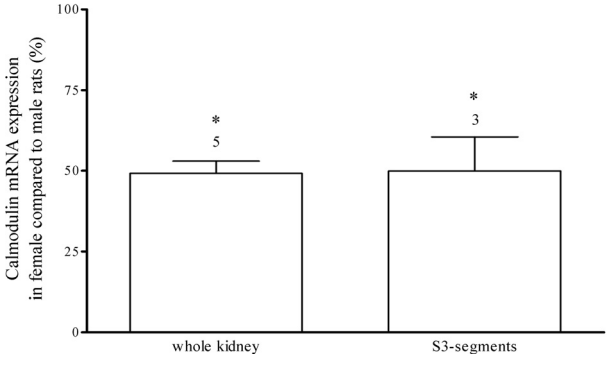

Figure 8. Real-time PCR analysis of calmodulin expression in whole kidneys and S3-segments from male and female rats. Results are expressed as percentage calmodulin expression in female compared to male rats. Gapdh expression was used as internal standard for normalization. Values are means ± SEM. The number of animals used is indicated above the columns; * indicates statistically significant different expression in female compared to male animals (unpaired t-test) ($P < 0.05$).

seem to be dependent on the number and position of phosphorylation sites in the transporter. A detailed description of the putative phosphorylation sites for PKC, PKA, PKG, and tyrosine kinase in the cloned OCT-isoforms can be found in [10].

Inhibition of CaM with calmidazolium resulted in a reduction of rOCT2 transport by 74%, indicating that the Ca^{2+}-CaM pathway is endogenously active in this expression system and stimulates rOCT2. A CaM dependent regulation of organic cation transport is also present in rOCT1 (G. Ciarimboli, unpublished data), hOCT1 [20], hOCT2 [19] and hOCT3 [22], showing that this regulation pathway is highly conserved within this transporter family. For this reason, we studied whether the calmodulin-associated regulation is related to change in K_m or V_{max} of the rOCT2. The comparison of saturation curves with or without calmodulin inhibition (Fig. 6b) suggests that calmodulin influences the K_m of the transporter, in contrast to that previously demonstrated for hOCT2, where calmodulin showed rather an effect on V_{max} [26]. A search of putative calmodulin binding sites in hOCT2 and rOCT2 using the calmodulin binding database of the Ikura Lab, Ontario Cancer Institute (http://calcium.uhnres.utoronto.ca/ctdb/ctdb/home.html) showed that hOCT2 has a putative calmodulin binding sequence at position 231–233. These sites in hOCT2 are localized in a short intracellular sequence linking transmembrane regions 4 and 5. Using a yeast two hybrid system where hOCT2 is the bait and calmodulin is the prey, we found no direct interaction of the two proteins (Ciarimboli et al., unpublished results). Rat OCT2 showed a putative calmodulin binding sequence between positions 299 and 304, corresponding to the big intracellular loop of the transporter. It is known that this loop in all the OCT isoforms contains several putative phosphorylation sites [10] and that changes in these sites are often associated with changes in apparent affinity of the transporter for its substrates [27]. These observations suggest that calmodulin does not interact directly with hOCT2, but possibly influences the trafficking of the transporter. On the other hand, calmodulin and/or a protein of its signalling pathway could directly interact with rOCT2, modifying its affinity.

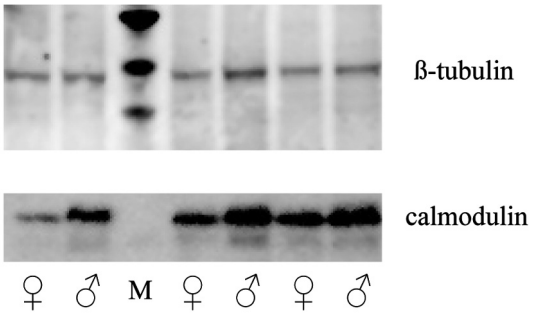

Figure 9a. Semi-quantitative Western blot analysis of calmodulin expression from male (♂) and female (♀) whole rat kidneys. ß-tubulin was used as internal standard. M indicates the lane with molecular weight markers. Calmodulin has an apparent molecular weight of around 20 kDa, ß-tubulin of around 55 kDa. Compared to females, male rat kidneys have a significantly higher renal expression of calmodulin.

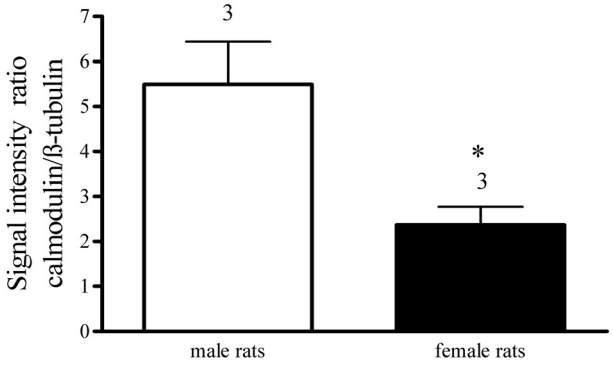

Figure 9b. Signal intensity ratios of calmodulin and ß-tubulin in male and female rat kidneys. Compared to females, male rat kidneys have a significantly higher renal expression of calmodulin (calmodulin/ß-tubulin quotient: 5.5 ± 0.9, $n = 3$ and 2.4 ± 0.4, $n = 3$, in male and female kidneys, respectively).

Furthermore, the effect of gender on rOCT2 regulation by CaM was investigated in freshly isolated S3-segments of proximal tubules from male or female rats in the absence of hormonal stimulation. Since this part of the nephron expresses mainly the rOCT2 [12], we could directly attribute the observed effects on basolateral ASP^+-accumulation to this OCT-isoform. In S3-segments from male rat kidneys, inhibition of CaM caused a significant reduction of rOCT2-mediated ASP^+-transport (Fig. 7b). Conversely, inhibition of CaM in freshly isolated S3-segments from female rat proximal tubules did not change the rOCT2-mediated ASP^+-transport, showing a gender-dependent post-translational regulation of OCT. The results of real-time PCR and of Western blot analysis show for the first time a gender-dependent expression of calmodulin. Oestrogens have been indeed shown to regulate the expression of several signalling molecules, such as CaMKII [35].

These findings show that the CaM pathway is of great importance in regulating OCT2 in male rats. Interestingly, cisplatin has been shown to be a substrate of rOCT2 and male rats appear to be more sensitive to cisplatin nephrotoxicity than female animals [36]. This finding has been put into relation with a lower OCT2 expression in female compared to male rats [36]. Additionally, since CaM endogenously activates rOCT2, a lower expression of CaM or of its downstream components, and therefore a lower rOCT2 activity, could render female renal cells less sensitive to

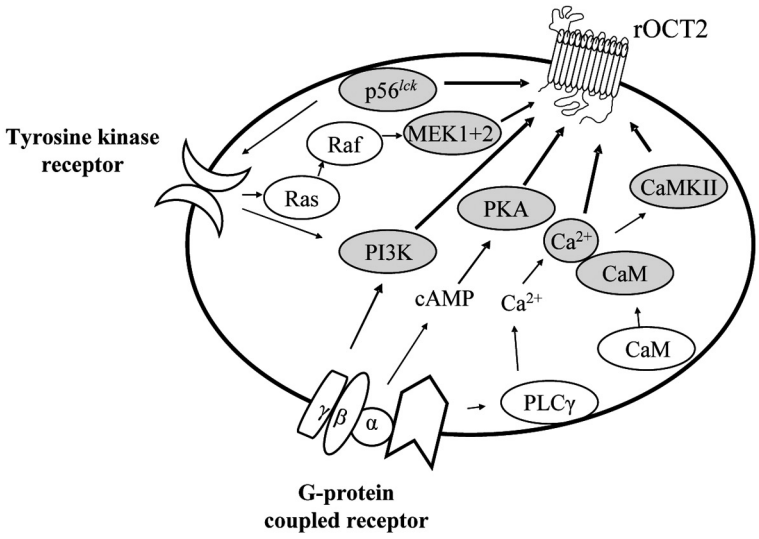

Figure 10. Schematic representation of rOCT2 regulation pathways identified in the present work. Grey circles indicate effective regulatory proteins. Bold arrows indicate a stimulation of rOCT2.

cisplatin toxicity. Indeed, there exists evidence that CaM is involved in modulation of cisplatin sensitivity [37]. Therefore, inhibition of CaM in proximal tubule cells expressing rOCT2 could decrease accumulation of cisplatin and hence associated nephrotoxicity. Because cisplatin is also a substrate for hOCT2 [5, 6], these correlations might lead to new options in reducing renal damage caused by chemotherapeutic therapy.

The CaM regulation pathway, effective in all OCTs, was confirmed to regulate OCT-mediated transport in the intact proximal tubule from rat kidney, accrediting relevance of results obtained in a cell system. This is the first study showing that post-translational regulation of rOCT2 is gender-dependent. These findings clearly show important differences both in acute and long-time regulation between the different OCT-isoforms and will be of high relevance in planning and interpreting further physiological and pharmacological investigations.

Acknowledgments. We thank Astrid Dirks for the excellent technical assistance. This work was supported by grants from the Deutsche Forschungsgemeinschaft (DFG Schl277/8–4) to ES, (DFG CI107/4–1) to GC and from the Innovative Medizinische Forschung of the Medical Faculty Münster (CI 120437) and the Else-Kröner-Fresenius-Stiftung (P56/06//A57/06) to GC.

1 Taubert, D., Grimberg, G., Stenzel, W., and Schomig, E. (2007). Identification of the endogenous key substrates of the human organic cation transporter OCT2 and their implication in function of dopaminergic neurons. PLoS ONE. 2, e385.
2 Ogasawara, M., Yamauchi, K., Satoh, Y., Yamaji, R., Inui, K., Jonker, J. W., Schinkel, A. H., and Maeyama, K. (2006). Recent advances in molecular pharmacology of the histamine systems: organic cation transporters as a histamine transporter and histamine metabolism. J. Pharmacol. Sci. 101, 24–30.
3 Shu, Y., Sheardown, S. A., Brown, C., Owen, R. P., Zhang, S., Castro, R. A., Ianculescu, A. G., Yue, L., Lo, J. C., Burchard, E. G. et al. (2007). Effect of genetic variation in the organic cation transporter 1 (OCT1) on metformin action. J. Clin. Invest. 117, 1422–1431.
4 Zhang, S., Lovejoy, K. S., Shima, J. E., Lagpacan, L. L., Shu, Y., Lapuk, A., Chen, Y., Komori, T., Gray, J. W., Chen, X. et al. (2006). Organic Cation Transporters Are Determinants of Oxaliplatin Cytotoxicity. Cancer Res. 66, 8847–8857.
5 Ciarimboli, G., Ludwig, T., Lang, D., Pavenstadt, H., Koepsell, H., Piechota, H. J., Haier, J., Jaehde, U., Zisowsky, J., and Schlatter, E. (2005). Cisplatin nephrotoxicity is critically mediated via the human organic cation transporter 2. Am. J. Pathol. 167, 1477–1484.
6 Yonezawa, A., Masuda, S., Yokoo, S., Katsura, T., and Inui, K. (2006). Cisplatin and oxaliplatin, but not carboplatin and nedaplatin, are substrates for human organic cation transporters (SLC22A1–3 and multidrug and toxin extrusion family). J. Pharmacol. Exp. Ther. 319, 879–886.
7 Chen, Y., Zhang, S., Sorani, M., and Giacomini, K. M. (2007). Transport of paraquat by human organic cation transporters and multidrug and toxic compound extrusion family. J. Pharmacol. Exp. Ther. 322, 695–700.
8 Busch, A.E., Karbach, U., Miska, D., Gorboulev, V., Akhoundova, A., Volk, C., Arndt, P., Ulzheimer, J. C., Sonders, M. S., Baumann, C. et al. (1998). Human neurons express the polyspecific cation transporter hOCT2, which translocates monoamine neurotransmitters, amantadine, and memantine. Mol. Pharmacol. 54, 342–352.
9 Koepsell, H., Schmitt, B. M., and Gorboulev, V. (2003). Organic cation transporters. Rev. Physiol. Biochem. Pharmacol. 150, 36–90.
10 Ciarimboli, G., and Schlatter, E. (2005). Regulation of organic cation transport. Pflugers Arch. 449, 423–441.
11 Okuda, M., Saito, H., Urakami, Y., Takano, M., and Inui, K. (1996). cDNA cloning and functional expression of a novel rat kidney organic cation transporter, OCT2. Biochem. Biophys. Res. Commun. 224, 500–507.
12 Karbach, U., Kricke, J., Meyer-Wentrup, F., Gorboulev, V., Volk, C., Loffing-Cueni, D., Kaissling, B., Bachmann, S., and Koepsell, H. (2000). Localization of organic cation transporters OCT1 and OCT2 in rat kidney. Am. J. Physiol. Renal Physiol. 279, F679-F687.
13 Urakami, Y., Okuda, M., Masuda, S., Akazawa, M., Saito, H., and Inui, K. (2001). Distinct characteristics of organic cation transporters, OCT1 and OCT2, in the basolateral membrane of renal tubules. Pharm. Res. 18, 1528–1534.
14 Motohashi, H., Sakurai, Y., Saito, H., Masuda, S., Urakami, Y., Goto, M., Fukatsu, A., Ogawa, O., and Inui, K. K. (2002). Gene expression levels and immunolocalization of organic ion

transporters in the human kidney. J. Am. Soc. Nephrol. 13, 866–874.
15 Urakami, Y., Nakamura, N., Takahashi, K., Okuda, M., Saito, H., Hashimoto, Y., and Inui, K. (1999). Gender differences in expression of organic cation transporter OCT2 in rat kidney. FEBS Lett. 461, 339–342.
16 Urakami, Y., Okuda, M., Saito, H., and Inui, K. (2000). Hormonal regulation of organic cation transporter OCT2 expression in rat kidney. FEBS Lett. 473, 173–176.
17 Asaka, J., Terada, T., Okuda, M., Katsura, T., and Inui, K. (2006). Androgen receptor is responsible for rat organic cation transporter 2 gene regulation but not for rOCT1 and rOCT3. Pharm. Res. 23, 697–704.
18 Mehrens, T., Lelleck, S., Cetinkaya, I., Knollmann, M., Hohage, H., Gorboulev, V., Boknik, P., Koepsell, H., and Schlatter, E. (2000). The affinity of the organic cation transporter rOCT1 is increased by protein kinase C-dependent phosphorylation. J. Am. Soc. Nephrol. 11, 1216–1224.
19 Cetinkaya, I., Ciarimboli, G., Yalcinkaya, G., Mehrens, T., Velic, A., Hirsch, J. R., Gorboulev, V., Koepsell, H., and Schlatter, E. (2003). Regulation of human organic cation transporter hOCT2 by PKA, PI3K, and calmodulin-dependent kinases. Am. J. Physiol. Renal Physiol. 284, F293-F302.
20 Ciarimboli, G., Struwe, K., Arndt, P., Gorboulev, V., Koepsell, H., Schlatter, E., and Hirsch, J. R. (2004). Regulation of the human organic cation transporter hOCT1. J. Cell. Physiol. 201, 420–428.
21 Soodvilai, S., Chatsudthipong, A., and Chatsudthipong, V. (2007). Role of MAPK and PKA in regulation of rbOCT2-mediated renal organic cation transport. Am. J. Physiol. Renal Physiol. 293, F21-F27.
22 Martel, F., Keating, E., Calhau, C., Gründemann, D., Schömig, E., and Azevedo, I. (2001). Regulation of human extraneuronal monoamine transporter (hEMT) expressed in HEK293 cells by intracellular second messenger systems. Naunyn-Schmiedeberg's Arch. Pharmacol. 364, 487–495.
23 Busch, A. E., Quester, S., Ulzheimer, J. C., Gorboulev, V., Akhoundova, A., Waldegger, S., Lang, F., and Koepsell, H. (1996). Monoamine neurotransmitter transport mediated by the polyspecific cation transporter rOCT1. FEBS Lett. 395, 153–156.
24 Arndt, P., Volk, C., Gorboulev, V., Budiman, T., Popp, C., Ulzheimer-Teuber, I., Akhoundova, A., Koppatz, S., Bamberg, E., Nagel, G. et al. (2001). Interaction of cations, anions, and weak base quinine with rat renal cation transporter rOCT2 compared with rOCT1. Am. J. Physiol. Renal Physiol. 281, F454-F468.
25 Pietig, G., Mehrens, T., Hirsch, J. R., Cetinkaya, I., Piechota, H., and Schlatter, E. (2001). Properties and regulation of organic cation transport in freshly isolated human proximal tubules. J. Biol. Chem. 276, 33741–33746.
26. Biermann, J., Lang, D., Gorboulev, V., Koepsell, H., Sindic, A., Schroter, R., Zvirbliene, A., Pavenstadt, H., Schlatter, E., and Ciarimboli, G. (2006). Characterization of regulatory mechanisms and states of human organic cation transporter 2. Am. J. Physiol. Cell. Physiol. 290, C1521-C1531.
27 Ciarimboli, G., Koepsell, H., Iordanova, M., Gorboulev, V., Dürner, B., Lang, D., Edemir, B., Schröter, R., van Le, T., and Schlatter, E. (2005). Individual PKC-phosphorylation sites in organic cation transporter 1 determine substrate selectivity and transport regulation. J. Am. Soc. Nephrol. 16, 1562–1570.
28 Schafer, J. A., Watkins, M. L., Li, L., Herter, P., Haxelmans, S., and Schlatter, E. (1997). A simplified method for isolation of large numbers of defined nephron segments. Am J Physiol 273, F650-F657.
29 Livak, K. J., and Schmittgen, T. D. (2001). Analysis of relative gene expression data using real-time quantitative PCR and the 2(-Delta Delta C(T)) Method. Methods 25, 402–408.
30 Nagel, G., Volk, C., Friedrich, T., Ulzheimer, J. C., Bamberg, E., and Koepsell, H. (1997). A reevaluation of substrate specificity of the rat cation transporter rOCT1. J. Biol. Chem. 272, 31953–31956.
31 Schmitt, B. M., and Koepsell, H. (2005). Alkali cation binding and permeation in the rat organic cation transporter rOCT2. J. Biol. Chem. 280, 24481–24490.
32 Schlatter, E., Mönnich, V., Cetinkaya, I., Mehrens, T., Ciarimboli, G., Hirsch, J. R., Popp, C., and Koepsell, H. (2002). The organic cation transporters rOCT1 and hOCT2 are inhibited by cGMP. J. Membr. Biol. 189, 237–244.
33 Gutkind, J. S. (1998). The pathways connecting G protein-coupled receptors to the nucleus through divergent mitogen-activated protein kinase cascades. J. Biol. Chem. 273, 1839–1842.
34 Kim, J. H., Chu, S. C., Gramlich, J. L., Pride, Y. B., Babendreier, E., Chauhan, D., Salgia, R., Podar, K., Griffin, J. D., and Sattler, M. (2005). Activation of the PI3K/mTOR pathway by BCR-ABL contributes to increased production of reactive oxygen species. Blood 105, 1717–1723.
35 Wong, K. A., Ma, Y., Cheng, W. T., and Wong, T. M. (2007). Cardioprotection by the female sex hormone – interaction with the beta(1)-adrenoceptor and its signaling pathways. Sheng Li Xue. Bao. 59, 571–577.
36 Yonezawa, A., Masuda, S., Nishihara, K., Yano, I., Katsura, T., and Inui, K. (2005). Association between tubular toxicity of cisplatin and expression of organic cation transporter rOCT2 (Slc22a2) in the rat. Biochem. Pharmacol. 70, 1823–1831.
37 Castagna, A., Antonioli, P., Astner, H., Hamdan, M., Righetti, S. C., Perego, P., Zunino, F., and Righetti, P. G. (2004). A proteomic approach to cisplatin resistance in the cervix squamous cell carcinoma cell line A431. Proteomics. 4, 3246–3267.